Available online at www.sciencedirect.com
SCIENCE DIRECT®
ELSEVIER
Mechanics Research Communications 31 (2004) 713–723
MECHANICS
RESEARCH COMMUNICATIONS
www.elsevier.com/locate/mechrescom

Dynamics of Timoshenko beams on Pasternak foundation under moving load

M.H. Kargarnovin*, D. Younesian

Center of Excellence in Design, Robotics and Automation, Mechanical Engineering Department, Sharif University of Technology, P.O. Box 11365-9567, Tehran, Iran

Available online 15 June 2004

Abstract

The response of a Timoshenko beam with uniform cross-section and infinite length supported by a generalized Pasternak-type viscoelastic foundation subjected to an arbitrary-distributed harmonic moving load is studied in this paper. Governing equations are solved using complex Fourier transformation in conjunction with the residue and convolution integral theorems. The solution is directed to compute the deflection, bending moment and shear force distribution along the beam length. A parametric study is carried out for an elliptical load distribution and influences of the load speed and frequency on the beam responses are investigated.

Keywords: Moving load; Vibration; Timoshenko beam; Viscoelastic foundation

1. Introduction

The dynamic response analysis of beams on viscoelasitc foundation under moving loads has been one of the research interests of railway engineers especially in last decades. So far and during these years many researchers have conducted different studies in this field. Fryba (1999) has presented some fundamentals in the dynamics of structures under moving load. Many authors (Achenbach and Sun, 1965; Grassie, 1982; Knothe and Grassie, 1993; Trochanis, 1987) have studied the steady state response of beams on a Kelvin viscoelastic foundation under a concentrated harmonic-moving load. In this paper the response of a uniform Timoshenko beam of infinite length placed on a viscoelastic foundation and subjected to an arbitrary distributed harmonic moving load is investigated. The speed and frequency of the moving load are assumed to be constant.

The mechanical model considered for the foundation is a generalized Pasternak viscoelastic model. This foundation model can be successfully used to simulate a newly-developed track support named ladder track system in which longitudinal sleepers are held together by transverse steel pipes and laid in parallel pairs under the rails (Mundrey, 2000). In this kind of viscoelastic model one set of parallel springs and dashpots

* Corresponding author.

0093-6413/$ - see front matter © 2004 Elsevier Ltd. All rights reserved.
doi:10.1016/j.mechrescom.2004.05.002

restricts any vertical displacement and another set, prevents the system from rocking motion. Furthermore, the existence of a shear viscous layer between beam and the foundation provides the interaction between these viscoelastic elements.

The governing differential equations are derived using Hamilton principle and are solved using complex Fourier transformation in conjunction with the residue and the convolution integral theorem. In performing numerical integration the shape of the distributive load can be in any arbitrary type however, in this paper it is assumed to be of the form of an elliptical function. The solution is directed to compute the deflection, bending moment and shear force along the beam length. Also, in this paper, effects of velocity and frequency variation of the load on the beam response are investigated.

2. Problem formulation

Fig. 1 illustrates a Timoshenko beam on a generalized Pasternak viscoelastic foundation under an arbitrary distributed harmonic-moving load. By using Hamilton principle and employing the Timoshenko beam theory, one can obtain the differential equations of the motion as (Kargarnovin and Younesian, 2001, 2002):

$$\rho A\frac{\partial^2 w(x,t)}{\partial t^2}+k^*AG\left(\frac{\partial\phi(x,t)}{\partial x}-\frac{\partial^2 w(x,t)}{\partial x^2}\right)-P_{\mathrm{f}}(x,t)=-Q(x,t) \tag{1}$$

$$EI\frac{\partial^2\phi(x,t)}{\partial x^2}-k^*AG\left(\phi(x,t)-\frac{\partial w(x,t)}{\partial x}\right)+M_{\mathrm{f}}(x,t)=\rho I\frac{\partial^2\phi(x,t)}{\partial t^2} \tag{2}$$

in which A, E, G, I, k^*, ρ, v, w, and ϕ are, cross-sectional area of the beam, the modulus of elasticity, shear modulus, cross-sectional moment of inertia, sectional shear coefficient, beam material density, load speed, beam deflection and beam slope due to bending, respectively. Moreover, Q represents the magnitude of distributed load, P_{f} and M_{f} are the foundation stimulated force and moment all per unit length of the beam and can be calculated as

$$P_{\mathrm{f}}(x,t)=-kw(x,t)-c\frac{\partial w(x,t)}{\partial t}+\mu\frac{\partial^3 w(x,t)}{\partial t\,\partial x^2} \tag{3}$$

$$M_{\mathrm{f}}(x,t)=-k_\phi\phi(x,t)-c_\phi\frac{\partial\phi(x,t)}{\partial t} \tag{4}$$

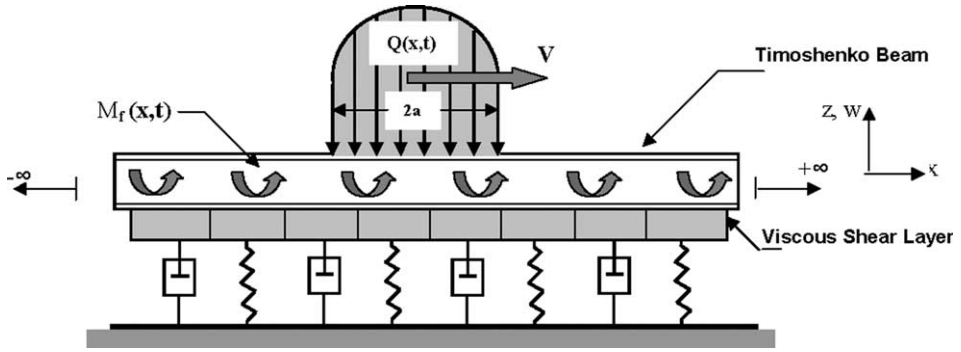

Fig. 1. A Timoshenko beam on viscoelastic foundation under moving load.

in which, k and c are foundation normal stiffness and damping coefficients, k_ϕ and c_ϕ are foundation rocking stiffness and damping coefficients and μ is the foundation shear viscosity coefficient.

In order to calculate the beam steady-state response, we use the following state variable transformation as

$$w_{\mathrm{st}}(s) = w(s)\,\mathrm{e}^{\mathrm{i}\omega t}, \qquad w(s) = w_A(s)\,\mathrm{e}^{\mathrm{i}\psi(s)} \tag{5}$$

$$\phi_{\mathrm{st}}(s) = \phi(s)\,\mathrm{e}^{\mathrm{i}\omega t}, \qquad \phi(s) = \phi_A(s)\,\mathrm{e}^{\mathrm{i}\theta(s)} \tag{6}$$

in which, $s = x - v\cdot t$, $w_A(s)$ and $\psi(s)$ are amplitude and phase of the steady state deflection and $\phi_A(s)$ and $\theta(s)$ are amplitude and phase of the slope due to bending and ω is the frequency of the moving load. After utilizing the differentiation chain rule on Eqs. (1) and (2) and considering Eqs. (5) and (6), one can get

$$Q(x,t) = Q_s(s)[H(s-a) - H(s+a)]\,\mathrm{e}^{\mathrm{i}\omega t} \tag{7}$$

$$\begin{aligned}&\rho A\left(v^2\frac{\mathrm{d}^2}{\mathrm{d}s^2} - 2\mathrm{i}\omega v\frac{\mathrm{d}}{\mathrm{d}s} - \omega^2\right)w(s) + k^*AG\left(\frac{\mathrm{d}\phi(s)}{\mathrm{d}s} - \frac{\mathrm{d}^2w(s)}{\mathrm{d}s^2}\right) - \mu\left(-v\frac{\mathrm{d}}{\mathrm{d}s} + \mathrm{i}\omega\right)\frac{\mathrm{d}^2w(s)}{\mathrm{d}s^2}\\ &\quad + c\left(-v\frac{\mathrm{d}}{\mathrm{d}s} + \mathrm{i}\omega\right)w(s) + kw(s) = -Q_s(s)[H(s-a) - H(s+a)]\end{aligned} \tag{8}$$

$$\begin{aligned}&EI\frac{\mathrm{d}^2\phi(s)}{\mathrm{d}s^2} - k^*AG\left(\phi(s) - \frac{\mathrm{d}w(s)}{\mathrm{d}s}\right) + c_\phi\left(v\frac{\mathrm{d}}{\mathrm{d}s} - \mathrm{i}\omega\right)\phi(s) + k_\phi\phi(s)\\ &\quad = \rho I\left(v^2\frac{\mathrm{d}^2}{\mathrm{d}s^2} - 2\mathrm{i}\omega v\frac{\mathrm{d}}{\mathrm{d}s} - \omega^2\right)\phi(s)\end{aligned} \tag{9}$$

It should be noted that the span of distributed moving load is $2a$ and H is the Heaviside function. Since the beam length is considered to be infinite hence, the boundary conditions are

$$\begin{cases}\underset{s\to\pm\infty}{\mathrm{Limit}}\, w(s) = \underset{s\to\pm\infty}{\mathrm{Limit}}\,\frac{\mathrm{d}w(s)}{\mathrm{d}s} = \underset{s\to\pm\infty}{\mathrm{Limit}}\,\frac{\mathrm{d}^2w(s)}{\mathrm{d}s^2} = 0\\ \underset{s\to\pm\infty}{\mathrm{Limit}}\,\phi(s) = \underset{s\to\pm\infty}{\mathrm{Limit}}\,\frac{\mathrm{d}\phi(s)}{\mathrm{d}s} = 0\end{cases} \tag{10}$$

The above boundary conditions represent this fact that at points far enough from the point of load application the central line deflection, its slope, concavity, shear force and bending moment are all approaching to zero.

3. Method of solution

In this paper in order to compute the response of the beam due to a distributive moving load, first we use the response of the beam under a concentrated moving load then compute the response of the beam to distributive load by use of convolution theorem. In other words, first we assume that $Q(x,t)$ is a unit Dirac delta function (δ_{D}) and compute the response of the beam using Fourier transformation. In this way we have

$$Q(x,t) = 1\times\delta_{\mathrm{D}}(s)\,\mathrm{e}^{\mathrm{i}\omega t} \tag{11}$$

Furthermore, we consider the complex Fourier transformation as

$$F(q) = \int_{-\infty}^{+\infty} f(s)\mathrm{e}^{-\mathrm{i}sq}\,\mathrm{d}s \tag{12}$$

After implementing the Fourier transform on Eqs. (8) and (9) and imposing the boundary conditions indicated in Eq. (10), $W_D(q)$ and $\Phi_D(q)$ are obtained as

$$W_D(q) = \frac{-(B_1q^2 + B_2q + B_3)}{B_4q^5 + B_5q^4 + B_6q^3 + B_7q^2 + B_8q + B_9} \tag{13}$$

$$\Phi_D(q) = \frac{(iB_{10}q)}{B_4q^5 + B_5q^4 + B_6q^3 + B_7q^2 + B_8q + B_9} \tag{14}$$

It should be mentioned that $W_D(q)$ and $\Phi_D(q)$ are Fourier transforms of $w(s)$ and $\phi(s)$, respectively.

Now, if an inverse Fourier transform is taken from both sides of Eqs. (13) and (14) then one will get

$$w_D(s^*) = \frac{1}{2\pi k r_0} \times \int_{-\infty}^{+\infty} \frac{-(B_1q^2 + B_2q + B_3)\, e^{is^*q}}{B_4q^5 + B_5q^4 + B_6q^3 + B_7q^2 + B_8q + B_9} dq \tag{15}$$

$$\phi_D(s^*) = \frac{1}{2\pi k r_0^2} \times \int_{-\infty}^{+\infty} \frac{(iB_{10}q)\, e^{is^*q}}{B_4q^5 + B_5q^4 + B_6q^3 + B_7q^2 + B_8q + B_9} dq \tag{16}$$

in which the coefficients B_1 to B_{10} are

$$B_1 = (\delta^2 - \beta^2), \qquad B_2 = (\eta\delta i - 2\omega^*\delta)$$

$$B_3 = (\omega^{*2} - \alpha^2 - \gamma - i\eta\omega^*), \qquad B_4 = -\lambda\delta(\delta^2 - \beta^2)i$$

$$B_5 = (\delta^2 - \beta^2)(\alpha^2 - \delta^2 + i\lambda\omega^*) + \delta^2\lambda(\eta + 2\omega^* i)$$

$$B_6 = (\delta^2 - \beta^2)(-\delta\xi i + 2\delta\omega^*) + (\delta\eta i - 2\omega^*\delta)(\alpha^2 - \delta^2 + i\lambda\omega^*) - \lambda\delta i(\omega^{*2} - \alpha^2 - \gamma - i\eta\omega^*)$$

$$B_7 = (\delta^2 - \beta^2)(1 - \omega^{*2} + i\xi\omega^*) + (\eta\delta i - 2\omega^*\delta)(-\xi\delta i + 2\omega^*\delta) + \alpha^4 + (\omega^{*2} - \alpha^2 - \gamma - i\eta\omega^*) \times (\alpha^2 - \delta^2 + i\lambda\omega^*)$$

$$B_8 = (\eta\delta i - 2\omega^*\delta)(1 - \omega^{*2} + i\xi\omega^*) + (\omega^{*2} - \alpha^2 - \gamma - i\eta\omega^*)(-\xi\delta i + 2\omega^*\delta)$$

$$B_9 = (\omega^{*2} - \alpha^2 - \gamma - i\eta\omega^*)(1 - \omega^{*2} + i\xi\omega^*)$$

$$B_{10} = \alpha^2$$

The dimensionless groups of parameters appeared in above relations are

$$s^* = sr_0^{-1}, \qquad a^* = ar_0^{-1}, \qquad r_0 = I^{0.5}A^{-0.5}, \qquad \alpha^2 = k^*GA^2k^{-1}I^{-1}$$

$$\beta^2 = EA^2k^{-1}I^{-1}, \qquad \lambda^2 = \mu^2I^{-2}Ak^{-1}\rho^{-1}, \qquad \gamma = k_\phi Ak^{-1}I^{-1}$$

$$\delta^2 = v^2A^2\rho k^{-1}I^{-1}, \qquad \xi^2 = c^2k^{-1}A^{-1}\rho^{-1}, \qquad \omega^* = \omega k^{-0.5}A^{0.5}\rho^{0.5}$$

$$\eta^2 = c_\phi^2 I^{-2}Ak^{-1}\rho^{-1}$$

To calculate integrals of Eqs. (15) and (16) it is necessary to employ the residue theorem. In this way we have for $w_D(s^*)$:

$$\int_{-\infty}^{+\infty} W_{\mathrm{D}}(q)\,\mathrm{e}^{\mathrm{i}s^*q}\mathrm{d}q = \pi\mathrm{i}\sum_{j_r=1}^{n_r}[\mathrm{Res}\ W_{\mathrm{D}}(z)\,\mathrm{e}^{\mathrm{i}s^*z}]_{z=z_{jr}} + 2\pi\mathrm{i}\sum_{j=1}^{n}[\mathrm{Res}\ W_{\mathrm{D}}(z)\,\mathrm{e}^{\mathrm{i}s^*z}]_{z=z_j}, \quad s^* \geqslant 0 \tag{17}$$

and

$$\int_{-\infty}^{+\infty} W_{\mathrm{D}}(q)\,\mathrm{e}^{\mathrm{i}s^*q}\mathrm{d}q = -\pi\mathrm{i}\sum_{j_r=1}^{n_r}[\mathrm{Res}\ W_{\mathrm{D}}(z)\,\mathrm{e}^{\mathrm{i}s^*z}]_{z=z_{jr}} - 2\pi\mathrm{i}\sum_{k=1}^{n}[\mathrm{Res}\ W_{\mathrm{D}}(z)\,\mathrm{e}^{\mathrm{i}s^*z}]_{z=z_k}, \quad s^* < 0 \tag{18}$$

in which, z_j represent the poles of $w_{\mathrm{D}}(z)$ in the upper half, z_k represent the poles of $w_{\mathrm{D}}(z)$ in lower half part of the complex plane and z_{jr} represent the real poles of $w_{\mathrm{D}}(z)$. In order to calculate the residue in jth pole of order mth one can use the following relation:

$$\mathrm{Res}[W_{\mathrm{D}}(z)\,\mathrm{e}^{\mathrm{i}sz}] = \frac{1}{(m-1)!}\lim_{z\to z_j}\frac{\mathrm{d}^{m-1}}{\mathrm{d}z^{m-1}}[(z-z_j)^m W_{\mathrm{D}}(z)\,\mathrm{e}^{\mathrm{i}sz}] \tag{19}$$

The same way of integration can be used for calculation of $\phi_{\mathrm{D}}(s^*)$. Then in order to calculate the bending moment and shear force, we can use following relations (Kargarnovin and Younesian, 2001, 2002):

$$M_{\mathrm{D}}(s^*) = r_0\beta^2\frac{\mathrm{d}\phi_{\mathrm{D}}(s^*)}{\mathrm{d}s^*} \tag{20}$$

$$V_{\mathrm{D}}(s^*) = \alpha^2\left[\phi_{\mathrm{D}}(s^*) - \frac{\mathrm{d}w_{\mathrm{D}}(s^*)}{\mathrm{d}s^*}\right] \tag{21}$$

Now, we use convolution integral theorem for computation of the response of the beam to distributive moving load. In this way we have:

$$w(s^*) = r_0\int_{-a^*}^{+a^*} Q_{s^*}(u)w_{\mathrm{D}}(s^*-u)\,\mathrm{d}u \tag{22}$$

$$M(s^*) = r_0\int_{-a^*}^{+a^*} Q_{s^*}(u)M_{\mathrm{D}}(s^*-u)\,\mathrm{d}u \tag{23}$$

$$V(s^*) = r_0\int_{-a^*}^{+a^*} Q_{s^*}(u)V_{\mathrm{D}}(s^*-u)\,\mathrm{d}u \tag{24}$$

The above integrals cannot be computed easily and it is necessary to employ one of the appropriate numerical methods of integration. In this paper, Gaussian quadrature method is employed.

It is important to mention that in the above-presented method of computation of the response of the beam, any kind of mathematical function for $Q_{s*}(u)$ in Eqs. (22)–(24) can be used.

4. Parametric study

In this paper, Q_{s^*} is taken to be an elliptical function. Note that elliptical function is one of the widely used mathematical functions in the contact analysis. Therefore, the general form of Q_{s^*} would be

$$Q_{s^*}(s^*) = Q_0\sqrt{a^{*2} - s^{*2}} \tag{25}$$

The data for a standard track (Trochanis, 1987, 2000) is

$\alpha = 50.4063$, $\beta = 139.39$, $\lambda = 5.9410$, $\xi = 0.2725$
$\gamma = 10.9025$, $\eta = 2.9705$, $k = 20$ MPa, $r_0 = 0.0677$ m

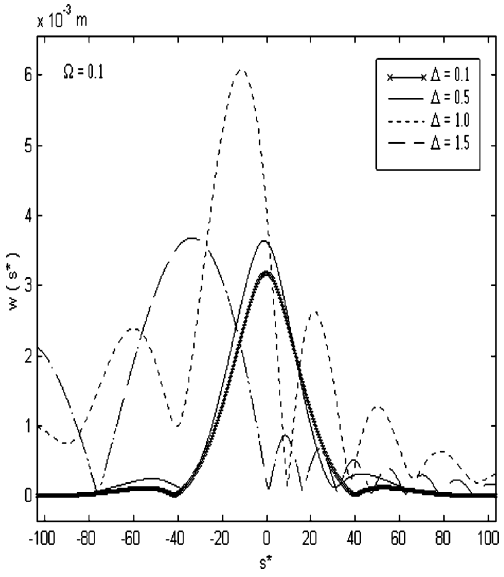

Fig. 2. Velocity effect on the deflection distribution.

We introduce two other new parameters namely Δ and Ω which are

$$\Delta = \frac{\delta}{\delta_{cr}}, \qquad \Omega = \frac{\omega^*}{\omega^*_{cr}} \tag{26}$$

δ_{cr} and ω^*_{cr} are critical value of dimensionless speed and frequency in which Euler–Bernoulli beam on Winkler foundation loses its stability (Fryba, 1999). For a track which is defined with above parameters δ_{cr} and ω^*_{cr} are calculated and their values are 16.6967 and 1.0, respectively. In order to complete the required values for different parameters we chose 5.0 and 14.46 kN/m for the a^* and Q_0, respectively in our simulation.

By using above values for different parameters, the integration procedure is pursued and the distribution of the displacement, bending moment and shear force along the beam length are calculated. Moreover, in this paper effects of the load velocity and frequency on the beam response are investigated.

Figs. 2, 5 and 8 illustrate the variation of displacement, bending moment and shear force under velocity change and Figs. 3, 6 and 9 represent the same variation but under frequency change. Also, in Figs. 4 and 7 variation of the maximum displacement and maximum bending moment by changing the value of load velocity and frequency are shown.

5. Results

Making use of the theoretical analysis described in the previous sections and in order to assess the effects of speed and frequency of the moving load on the amplitude of deflection, bending moment and shear force distribution, a parametric study is conducted as following. The variation of the beam deflection by changing of the load speed is illustrated in Fig. 2. It can be seen by increasing the speed of moving load, primarily the maximum deflection increases and then decreases. Moreover, this will cause the position of maximum deflection moves farther back with respect to the position of point ($s^* = 0$). Also, it can be seen that the number of apparent local peaks increases with increasing the load speed.

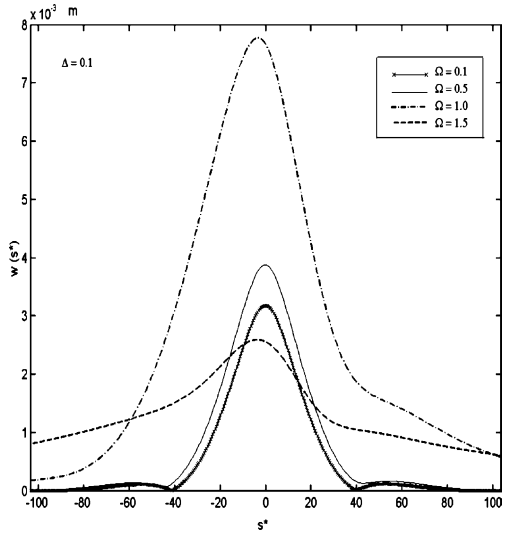

Fig. 3. Frequency effect on the deflection distribution.

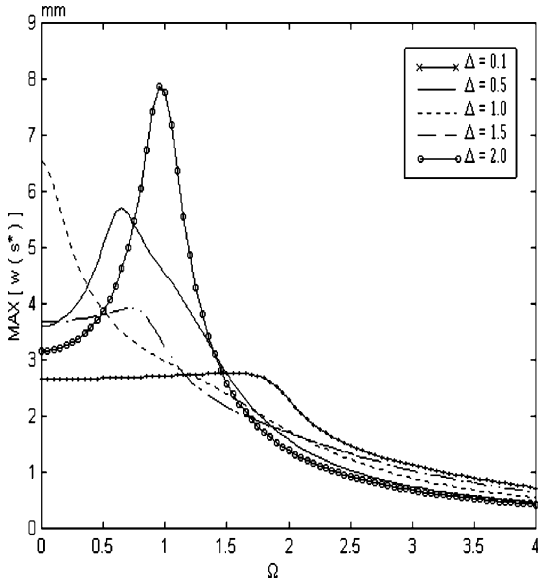

Fig. 4. Velocity and frequency effect on the maximum of deflection.

The effect of load frequency on the beam deflection is shown in Fig. 3. This effect is similar to the effect of speed increase on the beam deflection.

The effect of load frequency and speed on the maximum deflection is illustrated in Fig. 4. As it is seen in this figure, for speeds less than critical speed ($\Delta = 1$), by increasing load frequency the maximum deflection increases and after reaching to a maximum value it decreases. The frequency in which the peak of maximum deflection is reached (Ω_{peak}), depends on the value of the load speed. By increasing the value of speed, the difference of this frequency (Ω_{peak}), with the critical frequency ($\Omega = 1$) will be broadened and the peak value

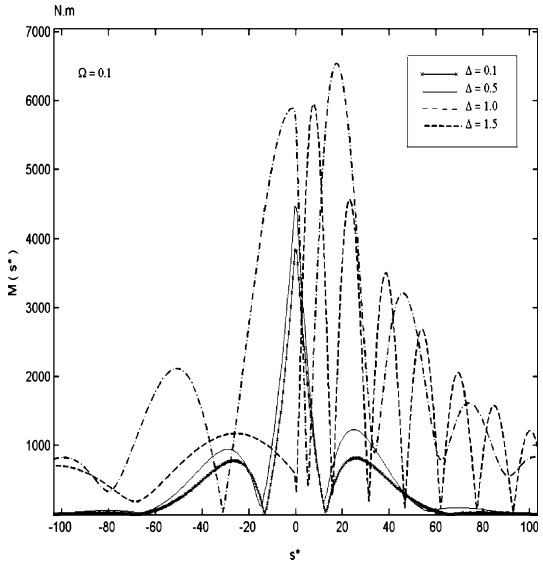

Fig. 5. Velocity effect on the bending moment distribution.

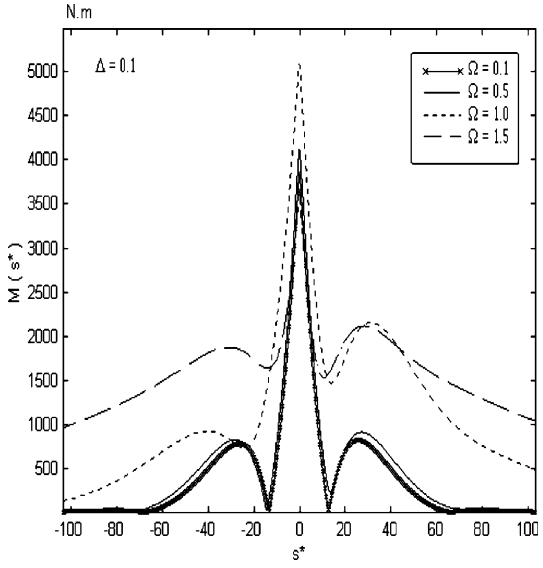

Fig. 6. Frequency effect on the bending moment distribution.

of the maximum deflection primarily decreases and then increases. Now, for the load speeds equal to the critical value, the maximum deflection decays by increasing the load frequency and for the speeds higher than critical speed the maximum deflection primarily indicates a growing trend and it decreases afterward.

The effect of load speed on the bending moment distribution is illustrated in Fig. 5. Any increases in the value of the load speed up to the critical value will cause the point of maximum bending moment moves to a point in front of point ($s^* = 0$). In the same figure for the speeds more than critical speed, the point of

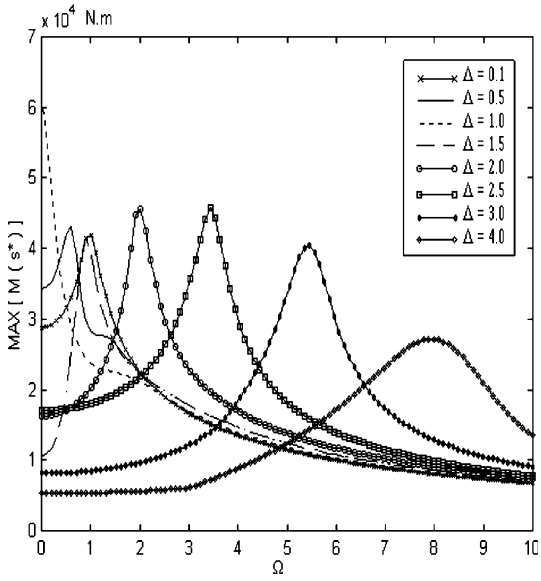

Fig. 7. Velocity and frequency effect on the maximum of bending.

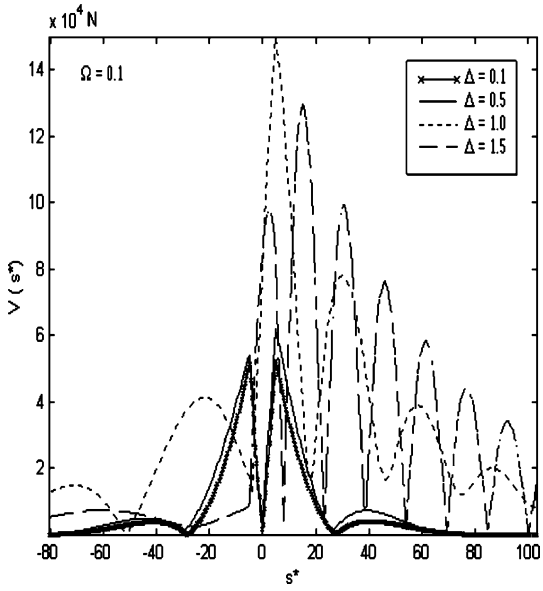

Fig. 8. Velocity effect on the shear force distribution.

maximum bending moment moves back and approaches again the to point ($s^* = 0$). In this case primarily the value of maximum bending moment increases and then decreases.

The effect of load frequency on the bending moment distribution is shown in Fig. 6. Any increases in the value of the load frequency have no effect on the location of the maximum bending moment. In this case primarily the value of maximum bending moment increases and then decreases.

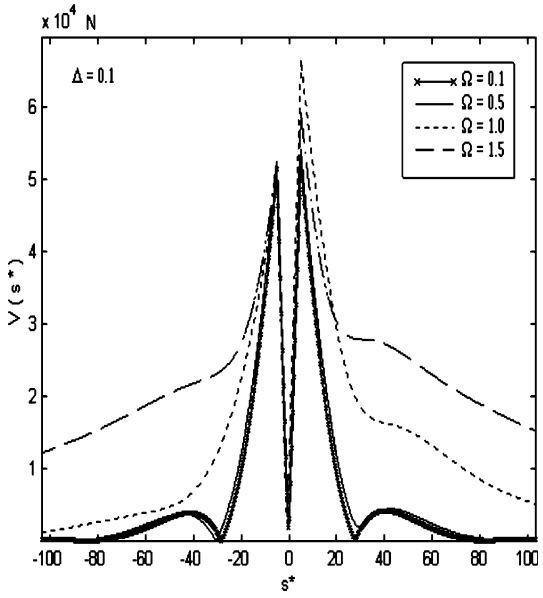

Fig. 9. Frequency effect on the shear force distribution.

The effect of load frequency and speed on the maximum bending moment is illustrated in Fig. 7. As it is seen in this figure, for speeds less than critical speed ($\Delta = 1$), by increasing the load frequency the maximum bending moment increases and after reaching to a maximum value it decreases. The frequency in which the peak of maximum bending moment is reached (Ω_{peak}), depends on the value of the load speed. By increasing the value of speed, the difference of this frequency (Ω_{peak}), with the critical frequency ($\Omega = 1$) will be broadened and the peak value of the maximum bending moment increases up to critical speed. Now, for the load speeds equal to the critical value, the maximum bending moment decays by increasing the load frequency. Note that for the case ($\Delta > 1$), the peak value of maximum bending moment primarily increases (up to $\Delta = 2.5$) and then decreases.

The effect of load speed on the shear force distribution is illustrated in Fig. 8. Similar trend as discussed for the bending moment can be seen in this figure. Also, it can be seen that the location of the peak value of shear forces stays at the end of the load span.

The effect of load frequency on the shear force distribution is shown in Fig. 9. It can be seen that any increases in the value of the load frequency have no effect on the location of the maximum shear force. Also, in this case primarily the value of maximum shear force increases and then decreases.

6. Conclusions

In this paper, to simulate the rail vibration due to a moving train, the response of a uniform Timoshenko beam of infinite length placed on a Pasternak viscoelastic foundation and subjected to a harmonic arbitrary distributed moving load was studied.

The solution of equations of motion resulted in, the distribution of deflection, bending moment and shear force along the beam length. Needless to say that these parameters are the most significant factors in the design of rail and its foundation in view of stress analysis in the rail and foundation, passenger comfort and noise generation. Since the presented results are in the non-dimensional form, they can be easily used in

a wide rang of practical cases. Moreover, in this paper, effects of changing the load velocity and frequency on the maximum values of beam responses were investigated. It was seen that variation of theses values vs. the velocity is also similar to the frequency response and follows the same trend as frequency response of a 1 DOF system.

Furthermore, it was seen that for each velocity there is a critical frequency in which the maximum deflection and bending moment are in their highest level. It should be mentioned that theses two critical frequencies are independent of each other and variation of the maximum bending moment and deflection vs. load frequency follow different trend. Also, it was demonstrated that unrelated to the level of load frequency, for the case of critical speed ($\Delta = 1.0$), we will have the highest maximum bending moment along the beam. In practical scene, it means that in the corrugated rails in which load velocity and frequency are not independent, the critical bending moment arises in critical speed independent of the wavelength of the corrugations. For the case of deflection, given a specified corrugation wavelength, the critical velocity can easily be calculated using one of the illustrated figures in this paper (Fig. 4).

References

Achenbach, J.D., Sun, C.T., 1965. Dynamic response of beam on viscoelastic subgrade. J. Eng. Mech. Div. 91.

Fryba, L., 1999. Vibration of Solids and Structures Under Moving Loads. Thomas Telford, London.

Grassie, S.L. et al., 1982. The Dynamic response of railway track to high frequency vertical excitation. J. Eng. Mech. 24 (2), 77.

Kargarnovin, M.H., Younesian, D., 2001. Dynamic analysis of Timoshenko beams on viscoelastic foundation under moving concentrated oscillating load. In: Proc. of the 5th Int. Conf. on Mechanical Engineering, Iran, p. 139.

Kargarnovin, M.H., Younesian, D., 2002. Dynamic response analysis of Timoshenko beam on viscoelastic foundation under an arbitrary distributed harmonic moving load. In: Proc. of the 4th Int. Conf. on Structural Dynamics, Germany, p. 875.

Knothe, K., Grassie, S.L., 1993. Modelling of railway track and vehicle/track interaction at high frequencies. Veh. Sys. Dyn. 22, 209.

Mundrey, J.S., 2000. Railway Track Engineering. Tata McGraw-Hill, New Delhi.

Trochanis, A.M. et al., 1987. Unified approach for beams on elastic foundations under moving loads. J. Geo. Eng. 113, 879.